INDICE

Low-cost travels within the Solar system

ALESSANDRA CELLETTI (*)

1. – Introduction

Launch a spacecraft from the Earth, get it in the deep space - closer to the Sun, leave the spacecraft for a while on an unstable equilibrium point (the same of having the spacecraft on the upper tip of a pendulum), catch the solar wind there and, blowing with the wind, come back home.

It could seem a science fiction story, but it is indeed reality. The spacecraft is called *Genesis*, a NASA sample return mission. Launched from Cape Canaveral on 8 August 2001, Genesis collected the solar wind at about 1,500,000 km from the Earth and brought the sample back, crashing on the desert floor in Utah (USA) on 8 September 2004.

The ambitious goal of collecting the wind of our star was complemented by another fascinating aspect: Genesis was placed in orbit around the *unstable equilibrium Euler-Lagrangian point*, known with the initials L_1. To understand where Genesis was located and how the mission was made possible, we need to jump in time back of two centuries and start a long story up to modern times, having as main characters three outstanding mathematicians: Leonhard Euler, Joseph–Louis Lagrange ([1]), Charles C. Conley.

1.1 – *Euler and Lagrange: a mere curiosity*

Among the outstanding contributions in several fields of mathematics, Leonhard Euler made in 1762 a seminal discovery in Celestial

(*) A.C. was partially supported by PRIN-MIUR 2010JJ4KPA_009, GNFM-INdAM and by the European Grant MC-ITN Astronet-II.

([1]) Although Lagrange is best known with the French version of his name, he was born in Turin, Piedmont, Italy, and the exact name was Giuseppe Lodovico Lagrangia.

echanics ([7]). He considered a three-body problem composed by oint-mass particles subject to the mutual gravitational influence. The stem was assumed to be formed by two main bodies, called the primaries, moving on circular orbits around their common barycenter, and small body orbiting between them; the small body was assumed not to fluence the motion of the primaries. Euler discovered three special nfigurations in which the three bodies keep always moving on the me line and maintaining the mutual distances unaltered. It must be ressed that each particle moves on its own orbit, although the three odies are aligned and at fixed distance at any time. The solutions found Euler are known as *collinear* equilibrium points and are typically enoted as L_1, L_2, L_3 (L_1 lies between the primaries, while L_2 and L_3 are cated beyond the primaries). The collinear equilibrium positions are own to be *unstable;* as we will see, this feature will play a relevant role invent low-cost missions, which exploit the instability of the collinear uilibria to move according to the *natural* dynamical laws and without king for fuel consumption.

A few years later, Lagrange discovered two more equilibrium nfigurations of the three–body problem ([18]), known as L_4 and L_5. ecisely, in a frame of reference rotating with the same angular vecity of the primaries around their common barycenter, a so–called *nodic* reference frame, one can find two equilibrium positions forming an equilateral triangle with the two primaries. Again, the three odies move on their own orbits, but in the synodic reference frame the uilateral configuration is permanently preserved. Unlike the colnear points, the triangular positions are shown to be stable for a wide nge of the mass-ratios of the primaries.

Although raved by his fantastic discovery, Lagrange was not conced that real bodies could move in such peculiar configurations with equilateral triangle shape. This is why he concluded that "Cette cherche n'est à la vérité que de pure curiosité" ([18]). Humankind ll need to wait about a century to discover real objects around the o triangular Lagrangian points of the Jupiter–Sun system. Inspired the Trojan war mythology, the two groups of asteroids are named ojan asteroids (located at L_5 and following Jupiter on its orbit, since ey lost the war) and Greek asteroids (located at L_4 and preceding Jupiter, being the winners). It must be noted that, due to an initial hesitation in the assignment of the names, the asteroids 617 Patroclus and 624 Hector belong to the enemies' group ([2]).

1.2 – *Conley: how knowledge will be applied*

Charles C. Conley gave seminal contributions in Dynamical Systems theory. Among the others, a remarkable result concerns the homotopy index theory, hence the name of *Conley index,* to investigate the topological properties of invariant sets ([6]). After having worked for some time as consultant for NASA, Conley wrote a visionary paper ([4], see also [5]), where he provided new concepts to travel within the Solar system at low-cost. The first ingredient of his paper is the use of the collinear points in the three-body problem, since – as we mentioned before – one can take advantage of their instability. The second ingredient is a suitable version of Lyapunov's theorem provided by J. Moser, who was the Ph.D. advisor of Conley; this theorem ensures that the results obtained within the linearized setting are valid also in the nonlinear framework ([19]). Combining these ingredients, he was able to prove the existence of *transit* orbits between the primaries for suitable energy levels.

In the last part of his paper Conley studies an example in which the primaries are the Earth and the Moon, and he provides the design of a mission with the requisites to be low-cost and flexible. The price to pay is that to go from the Earth to the Moon without consuming too much fuel and just exploiting the routes of chaos, one needs a time which is much longer with respect to the 3 days that the Apollo 11 required in 1969 to bring the first astronauts on the Moon. This remark justifies one of the final sentences of Conley's paper about the use of transit orbits around the collinear points: "Unfortunately, orbits such as this

([2]) Objects in the triangular Lagrangian positions L_4 and L_5 are usually referred to as simply *Trojans,* without making a distinction between Greeks and Trojans. Trojan objects are found also around the Earth, Mars, Uranus and Neptune. An updated list is maintained by the Minor Planet center at http://www.minorplanetcenter.net/iau/lists/Trojans.html

quire a long time to complete a cycle (e.g., 6 months, though a mo-
ication of the notion might improve that)".
However, he also added a sentence that leaves a ray of hope as far as
ssible applications of his ideas in Astrodynamics are concerned;
ecisely, he stated that "One cannot predict how knowledge will be
plied – only that it often is".
The prediction will soon be verified, thus becoming a paradigm of
w mathematical ideas are often applied in concrete problems.

3 – *Interplanetary highways*

It was necessary to wait only 10 years to see that Conley's new ideas
Astrodynamics can be applied in a very effective way. The first
ssion using the collinear points was the NASA/ESA "International
n/Earth Explorer 3", known with the acronym ISEE-3; launched in
78, it was initially placed on a periodic orbit around the collinear
int L_1 between the Earth and the Sun to monitor the Earth's in-
planetary medium. In 1982 the spacecraft was moved to transfer
bits between the Earth and the collinear point L_2, before being
cted by the Earth–Moon system in order to travel on a trajectory
king a rendezvous with the Giacobini-Zinner comet in 1985.
After ISEE-3 an increasing number of space missions have been
signed taking advantage of the peculiarities of the collinear points
e Section 6, compare with [11], [17]). Nowadays, the branch of
trodynamics using the concepts of Dynamical Systems to design
ace missions is so wide that it deserves a specific name and it is
nmonly known as *Space Manifold Dynamics.*
The missions to which we will refer in Section 6.2 exploit the
tures of the collinear points, but also the triangular positions can
effectively used to place a spacecraft. Indeed, the triangular po-
ons L_4 and L_5 came to the fore much earlier then the space ex-
ration era, precisely when the first asteroid, 588 Achilles, was
nd to orbit on a triangular position by the astronomer M. Wolf. It
s the year 1906 and nowadays more than 6 000 asteroids (com-
nly known as Trojan asteroids) are currently known to move in
triangular points L_4 or L_5.

As a conclusion of the whole story, let us say that although the triangular positions seemed to Lagrange quite exotic and the collinear points were for Conley possibly inappropriate in space missions, the development of science tells us that what might seem just a mathematical curiosity, without practical consequences, can have indeed spectacular applications.

This paper is organized as follows. The basic of Astrodynamics is given by Kepler's laws, which are discussed in Section 2. The Keplerian ellipses can be used to transfer probes between two bodies, e.g. the Earth and the Moon; these are the so-called Hohmann transfers presented in Section 3. In passing from the Keplerian 2-body problem to the more complicated 3-body problem, the increasing complexity is compensated by the discovery of the Euler-Lagrange equilibrium solutions in the rotating reference frame as presented in Section 4. The features of the equilibrium solutions which are collinear with the primaries are studied in Section 5. The peculiarities of the collinear points are finally exploited to design low-energy missions as described in Section 6.

2. – Kepler's laws

Johannes Kepler (1571-1630) laid the foundations of orbital dynamics by means of three laws which bring his name. Kepler worked as assistant of the Danish astronomer Tycho Brahe (1546-1601). Thanks to the generosity of the King of Denmark and Norway Frederik II, Brahe was able to build an astronomical observatory on the Hven island in Sweden. The observatory was called *Uraniborg* and it had an underground facility called *Stjerneborg,* the star castle. By using his very elaborated astronomical instruments, Tycho Brahe was able to collect very accurate data about the position of stars and planets. These data were later analyzed by Kepler to determine the laws governing the celestial motions. It is remarkable that Kepler discovered such laws without knowing about the existence and properties of the force acting between the celestial bodies, since the gravitational law was formulated by Isaac Newton in his "Philosophiæ Naturalis Principia Mathematica", published only in 1687, well beyond Kepler's death.

Within the approximation of the *2-body problem*, namely a model omposed by two bodies moving under the mutual gravitational attraction (e.g., a planet and the Sun), Kepler formulated three laws that ell us on which trajectories the planets move (they are elliptic orbits), ow these trajectories are span by the bodies and, finally, where the rbits are located according to their revolution times.

The *first Kepler's law* states that the planets move on ellipses round the Sun and our star is placed in one of the two foci of the ellipse when applied to artificial satellites, the first law states that the spaecraft moves on an ellipse with the Earth at one of its foci). The dicovery of elliptic orbits was announced in the "Astronomia Nova", vhere Kepler stated "hic quasi e somno expergefactus, et novam lucem ntuitus, sic cœpi ratiocinari" ([3]).

According to *second Kepler's law* (see [16]), along the ellipse the ody sweeps equal areas in equal times. This law is also known as the *aw of areas*, and its consequence is that the bodies move faster at eriastrum (namely, the point on the ellipse closer to the primary) and low down at apoastrum (that is, the point farther from the primary).

The *third Kepler's law* relates the semimajor axis a of the ellipse vith the period T of motion, according to the following formula (in suitable units of measure, precisely in years for the period and in Astronomical Units ([4]) for the semimajor axis):

$$T^2 = a^3 \,. \tag{2.1}$$

As a consequence, the bigger is the distance of the celestial body from he primary, the longer is the time necessary to complete a full orbit. As we will see later, the third law, formulated in Chapter 5 of Kepler's masterpiece "Harmonices Mundi", has many practical consequences and will help us to understand how long an interplanetary travel might be. Before turning to Astrodynamics, it is worth exploring the power of

([3]) "Like suddenly awakened from sleep, and seeing a new light, thus I started to think" ([16]). The author thanks A. Giorgilli for letting her know about this sentence.

([4]) One Astronomical Unit (AU) is a measure of the average Earth–Sun distance and it is about equal to $1.5 \cdot 10^8$ km.

Kepler's third law by looking at the data provided in Table 2.1, which compares the values of the planetary semimajor axes as given by (2.1) with those measured by NASA as reported in [21]. It is immediate to realize that the agreement is remarkable especially for the bodies closer to the Sun.

TABLE 1. – Values of the semimajor axes of the planets computed from Kepler's third law (2.1) using the periods in the first column (see the second column) and values of the semimajor axes provided by NASA in [21] (see the third column). For fast reference, the figures in bold in the last column are those which agree with the values obtained by implementing Kepler's third law (2.1) in the second column.

	Period in years	Semimajor axis in AU from (2.1)	Semimajor axis in AU from [21]
Mercury	0.2408	0.3870	**0.38709927**
Venus	0.6152	0.7233	**0.72333566**
Earth	1	1	**1**
Mars	1.8808	1.5237	**1.52371034**
Jupiter	11.8626	5.2014	**5.20288700**
Saturn	29.4475	9.5360	**9.53667594**
Uranus	84.0168	19.1827	**19.18916464**
Neptune	164.7913	30.0577	**30.06992276**

3. – Hohmann transfers

While designing a space mission, the first trivial consideration is that natural orbits are not straight lines (as one could naively think), but rather elliptic trajectories, shaped by gravity, namely by the attraction of the primary. This is why, although Kepler's laws are a well-known topic widely discussed in classical textbooks, a deep insight in the Astrodynamical concepts cannot leave aside the treatment of the laws ruling the 2-body problem. These basic laws were used in modern times to launch spacecraft, paying attention to reduce the costs as much as possible. The problem of traveling in space by minimizing the fuel consumption was thoroughly inve-

stigated by Walter Hohmann (1880-1945), who published in 1925 the treatise "Die Erreichbarkeit der Himmelskörper" ([14]). His ideas were extensively used in the Apollo programs as well in interplanetary missions.

Hohmann suggested the following strategy that we apply to the case of a spacecraft from Earth to Mars. Assume that the Earth and Mars move on circular orbits around the Sun, respectively labeled as 1 and 3 in Figure 1; a spacecraft leaving from the Earth can reach Mars by covering the semi-ellipse (labeled 2 in Figure 1) with focus in the Sun and semimajor axis equal to half of the sum of the radii of Earths' and Mars' circular orbits. A variation of the velocity (which corresponds to a fuel consumption) is necessary to place the spacecraft on the elliptic orbit; we will say that this maneuver costs ΔV_1. At the end, we will need a second maneuver to put the spacecraft along Mars' orbit and we will say that it costs ΔV_2. Rather than launching on a straight orbit from Earth to Mars, the Hohmann transfer orbit corresponding to the Keplerian (semi-)ellipse is the most natural trajectory with a very limited cost $\Delta V_1 + \Delta V_2$. Hohmann transfer orbits provide the basis of Flight Dynamics.

Kepler's third law allows us to estimate the time necessary to travel

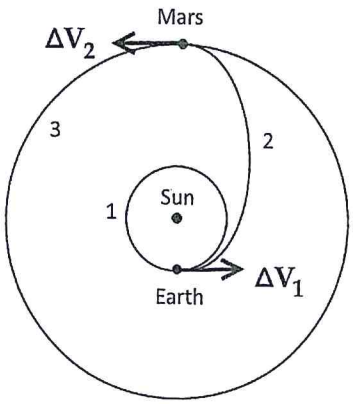

Fig. 1. – A Hohmann transfer from the Earth (circular orbit n. 1) to Mars (circular orbit n. 3) along the semi-ellipse n. 2. The fuel cost to insert the spacecraft on the right orbit is provided by the quantity $\Delta V_1 + \Delta V_2$.

from the Earth to Mars along a Hohmann transfer. In fact, given that the semimajor axes (that we assume equal to the radii of the circles) of Earth and Mars are, respectively, equal to 1 AU and 1.52 AU, the semimajor axis of the transfer ellipse is equal to $2.52/2 = 1.26\ AU$. From (2.1) we obtain that the period to run the semi-ellipse is equal to $T = \frac{1}{2}(1.26)^{\frac{3}{2}} = 0.707$ years (about 8.5 months). This is a realistic estimate of the time needed to reach Mars.

4. – The Euler-Lagrange equilibrium points

Things become very much complicated, when considering a model including the action of a third body. Unlike Kepler's two body problem, the three–body system becomes non–integrable and one cannot infer the existence of simple orbits like the Keplerian ellipses in the two–body framework. Nevertheless, some special solutions exist, precisely equilibrium solutions of the equations of motion in a reference frame, called *synodic frame*, rotating with the angular velocity of the primaries. To be precise, let $(\mathcal{O}, \xi, \eta, \zeta)$ denote a *sidereal* reference frame with origin coinciding with the barycenter of three–bodies $\mathcal{P}_1$, $\mathcal{P}_2$, $\mathcal{P}_3$, whose masses are, respectively, m_1, m_2, m_3 with $m_1 > m_3 \gg m_2$. The bodies $\mathcal{P}_1$ and $\mathcal{P}_3$ are called *primaries*, while $\mathcal{P}_2$ denotes a small body whose mass is much smaller than that of the primaries. We assume that the axes of the reference frame are oriented as follows: the ξ axis has the same direction of the line joining the primaries $\mathcal{P}_1$ and $\mathcal{P}_3$, the η axis is taken orthogonally in the orbital plane and the ζ axis is perpendicular to the orbital plane. Assume that the units of measure are such that the distance between $\mathcal{P}_1$ and $\mathcal{P}_3$ is equal to one and that $\mathcal{G}(m_1 + m_3) = 1$. Moreover, let $\overline{\mu} \equiv \dfrac{m_3}{m_1 + m_3}$, so that $\mu_1 \equiv \mathcal{G}m_1 = 1 - \overline{\mu}$, $\mu_3 \equiv \mathcal{G}m_3 = \overline{\mu}$.

We denote by (ξ_i, η_i, ζ_i) the coordinates of $\mathcal{P}_i$, $i = 1, 2, 3$, in the sidereal frame. The equations of motion of the small body $\mathcal{P}_2$ can be written as

$$
\begin{aligned}
\ddot{\xi}_2 &= \mu_1 \frac{\xi_1 - \xi_2}{r_1^3} + \mu_3 \frac{\xi_3 - \xi_2}{r_3^3} \\
\ddot{\eta}_2 &= \mu_1 \frac{\eta_1 - \eta_2}{r_1^3} + \mu_3 \frac{\eta_3 - \eta_2}{r_3^3} \\
\ddot{\zeta}_2 &= \mu_1 \frac{\zeta_1 - \zeta_2}{r_1^3} + \mu_3 \frac{\zeta_3 - \zeta_2}{r_3^3}
\end{aligned} \tag{4.1}
$$

with

$$
r_1 = \sqrt{(\xi_1 - \xi_2)^2 + (\eta_1 - \eta_2)^2 + (\zeta_1 - \zeta_2)^2} \,,
$$

$$
r_3 = \sqrt{(\xi_3 - \xi_2)^2 + (\eta_3 - \eta_2)^2 + (\zeta_3 - \zeta_2)^2} \,.
$$

Let $(\mathcal{O}, x, y, z)$ denote the *synodic* reference frame, which we assume to rotate with the angular velocity, say n, of the primaries around their common barycenter, where n has been normalized to one due to the choice of the units of measure. The x axis coincides with the direction joining the primaries, so that $\mathcal{P}_1$ and $\mathcal{P}_3$ lie at fixed positions with coordinates $(x_1, y_1, z_1) = (-\mu_3, 0, 0)$, $(x_3, y_3, z_3) = (\mu_1, 0, 0)$. By implementing the change of variables relating the sidereal and synodic frames:

$$
\begin{aligned}
\xi &= x \cos t - y \sin t \\
\eta &= x \sin t + y \cos t \\
\zeta &= z \,,
\end{aligned}
$$

and denoting by (x, y, z) the coordinates of $\mathcal{P}_2$ in the synodic frame, the equations of motion (4.1) become:

$$
\begin{aligned}
\ddot{x} - 2\dot{y} &= \frac{\partial U}{\partial x} \\
\ddot{y} + 2\dot{x} &= \frac{\partial U}{\partial y} \\
\ddot{z} &= \frac{\partial U}{\partial z} \,,
\end{aligned} \tag{4.2}
$$

where the function U is defined as

$$
U = U(x, y, z) \equiv \frac{1}{2}(x^2 + y^2 + z^2) + \frac{\mu_1}{r_1} + \frac{\mu_3}{r_3}
$$

with the distances transformed as

$$
r_1 = \sqrt{(x + \mu_3)^2 + y^2 + z^2} \,, \qquad r_3 = \sqrt{(x - \mu_1)^2 + y^2 + z^2} \,. \tag{4.3}
$$

From (4.3) and taking into account that $\mu_1 + \mu_3 = 1$, one obtains that $\mu_1 r_1^2 + \mu_3 r_3^2 = x^2 + y^2 + z^2 + \mu_1 \mu_3$, which provides for U the alternative expression:

$$
U = \mu_1 \left(\frac{r_1^2}{2} + \frac{1}{r_1} \right) + \mu_3 \left(\frac{r_3^2}{2} + \frac{1}{r_3} \right) - \frac{1}{2} \mu_1 \mu_3 \,. \tag{4.4}
$$

Then, from the equations of motion (4.2), multiplying the three equations respectively by $\dot{x}$, $\dot{y}$, $\dot{z}$, adding the results and integrating with respect to time one obtains the expression:

$$
\dot{x}^2 + \dot{y}^2 + \dot{z}^2 = 2U - C_J \,, \tag{4.5}
$$

where C_J is a constant called the *Jacobi integral*. Given (4.4) and (4.5), we get that the motion is allowed in the region satisfying the following constraint:

$$
2\left[\mu_1 \left(\frac{r_1^2}{2} + \frac{1}{r_1} \right) + \mu_3 \left(\frac{r_3^2}{2} + \frac{1}{r_3} \right) \right] - \tilde{C}_J \geq 0 \,, \tag{4.6}
$$

where $\tilde{C}_J \equiv \mu_1 \mu_3 + C_J$. For a fixed value of the Jacobi integral, the zero–velocity curve obtained by taking the equality in (4.6) is the boundary of a region, called *Hill's surface*, which separates the domain where the motion is allowed from that in which the motion is forbidden (see Figure 2).

Let us have a look at the last plot in Figure 2, which shows five equilibrium positions, namely the five stationary points of the potential in the synodic reference frame. Three positions, named L_1, L_2, L_3, are those discovered by Leonhard Euler and are called the *collinear* equilibrium points, since they lie along the line joining the primaries. The other two positions, L_4, L_5, are those found by Joseph-Louis Lagrange and are called the *triangular* equilibrium

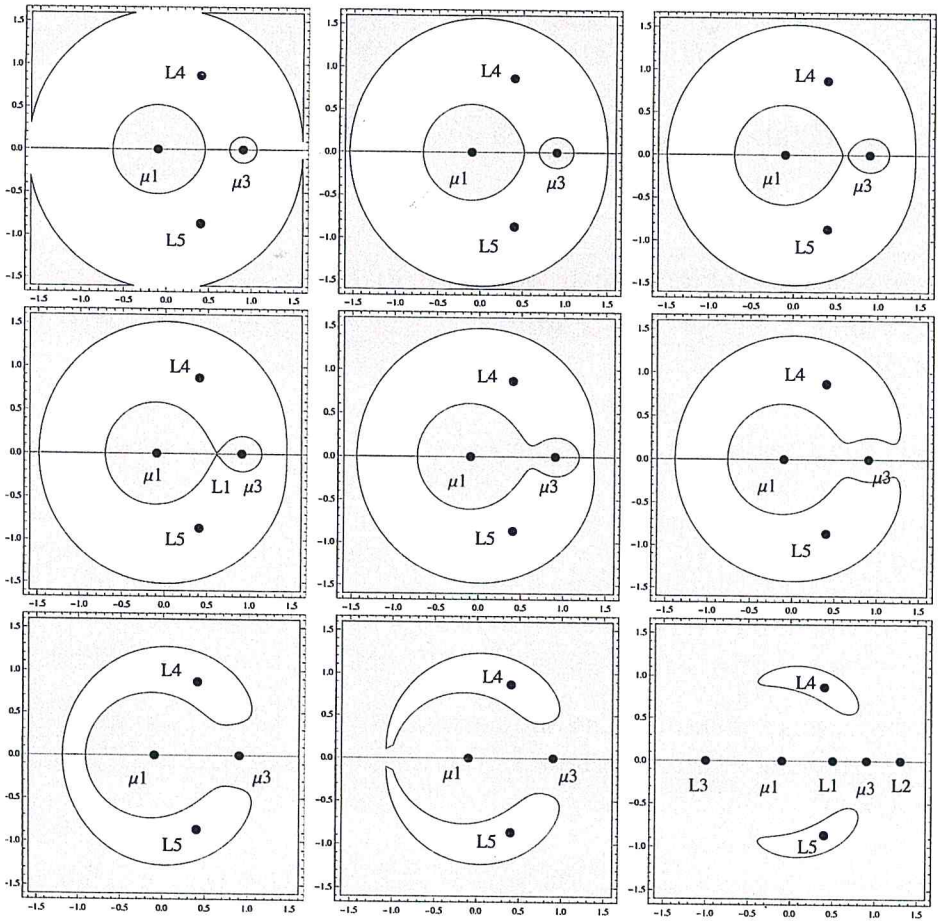

Fig. 2. – Hill's surfaces for $\mu_1 = 0.9$, $\mu_3 = 0.1$; the last plot shows the position of the triangular and collinear equilibrium points (all other plots show only the triangular points). The admissible region is marked in grey. From upper left to bottom right $\tilde{C}_J$: 4, 3.8, 3.7, 3.687, 3.6, 3.5, 3.25, 3.19284, 3.08.

points, since they form two equilateral triangles with the primaries (see, e.g., [2], [20] for the mathematical derivation of the collinear and triangular equilibria). The collinear points are unstable for any value of the mass–ratio of the primaries. The triangular points are stable, provided that the following bound on the mass of $\mathcal{P}_3$ is satisfied:

$$\mu_3 \leq \frac{27 - \sqrt{621}}{54} \simeq 0.0385 \ .$$

This value is greater than all planet–Sun mass–ratios as well as than the Moon–Earth mass–ratio, thus ensuring stability of the triangular positions in these cases. In the Moon–Earth system the point L_1 is located at $3.26 \cdot 10^5$ km from the Earth (for comparison the Moon is at $3.84 \cdot 10^5$ km), L_2 is at distance $4.49 \cdot 10^5$ km, L_3 at about $3.82 \cdot 10^5$ km from the Earth, while the Earth–Moon triangular positions lie on the orbit of the Moon, thus at a distance of $3.84 \cdot 10^5$ km from the Earth.

The plots shown in Figure 2 will be the centerpiece of the rest of our discussion. The remarkable observation is that the admissible regions are completely different as the energy level varies; in the upper plots, the motion is allowed only in some regions (with increasing size) around the primaries. In the left plot of the middle line the regions around the primaries touch at the Lagrangian point L_1. For lower values of $\tilde{C}_J$ the bottleneck at L_1 opens (see the center plot of the middle line). At the corresponding energy level a route from the two primaries is allowed and the minor body can travel through the bottleneck to reach both primaries. At all other values the extent of the admissible region increases considerably.

We stress that a slight change of $\tilde{C}_J$ around the value 3.687 makes a huge difference: for (even slightly) higher values the two primaries are isolated and a spacecraft can travel only around one of the primaries, without reaching the other; for (even slightly) smaller values of the Jacobi integral the spacecraft can leak through the small escape route connecting one body to the other.

5. – Around the collinear points

To explore the dynamics around the collinear points, we start by linearizing the equations of motion and by computing the corresponding eigenvalues (see Section 5.1). We anticipate the result by saying that for any of the three collinear points one finds 2 real eigenvalues (say $\pm\lambda$) and 4 imaginary eigenvalues (that we shall call

$= i\omega_2, \pm i\omega_3$). This means that the dynamics is of the type

$$saddle \times center \times center$$

nd it implies that in the neighborhood of the collinear points we find ıe composition of one hyperbolic behavior and two oscillators. Orbits round the collinear point L_1 can then be classified in different categories (see Section 5.2), which include also *transit* orbits: they allow ne to move from one primary to the other through the neck around ıe collinear point.

When dealing with the nonlinear approximation, we need to use Ioser's version of Lyapunov's theorem to establish that the results ɔund within the linearized framework are valid also in the context of ıe full nonlinear equations.

We can get rid of the instability due to the hyperbolic component by erforming a *center manifold reduction* (see Section 5.3) and we ɔnclude by defining different kinds of trajectories within such center ıanifold, known as *halo* and *Lissajous* orbits (see Section 5.4).

.1 – *The linearized flow*

To study the linearized flow, we adopt a procedure, which consists of vo main steps (details can be found, e.g., in [15], see also [22]). With eference to (4.2), the first one consists in computing a suitable change variables in order to shift and scale the equilibrium point. The seɔnd step aims at reducing the quadratic part of the Hamiltonian ınction to a simpler form: a diagonal form for the hyperbolic comɔnents and harmonic oscillators along the stable directions.

We skip the details which can be found for example in [15], [12], [3], ıd we provide the final result as follows. Using a suitable set of ɔordinates, say $q = (q_1, q_2, q_3)$, and associated momenta, say $p = ɔ_1, p_2, p_3)$, the Hamiltonian of the linearized flow around the collinear ɔints can be written as

$$H_{linear}(p,q) = \lambda p_1 q_1 + \frac{\omega_2}{2}(p_2^2 + q_2^2) + \frac{\omega_3}{2}(p_3^2 + q_3^2) \,, \tag{5.1}$$

where $\lambda, \omega_2, \omega_3$ are real positive quantities connected to the roots of the characteristic polynomial associated to the linearized matrix.

Hamilton's equations associated to (5.1) are given by

$$\begin{aligned} \dot{q}_1 &= \lambda q_1 & \dot{q}_2 &= \omega_2 p_2 & \dot{q}_3 &= \omega_3 p_3 \\ \dot{p}_1 &= -\lambda p_1 & \dot{p}_2 &= -\omega_2 q_2 & \dot{p}_3 &= -\omega_3 q_3 \,, \end{aligned}$$

with admit the solution:

$$q_1(t) = q_1(0)e^{\lambda t} \,, \qquad p_1(t) = p_1(0)e^{-\lambda t}$$

for the hyperbolic direction and

$$z_2(t) \equiv q_2(t) + ip_2(t) = z_2(0)e^{-i\omega_2 t} \,, \quad z_3(t) \equiv q_3(t) + ip_3(t) = z_3(0)e^{-i\omega_3 t}$$

for the center directions.

5.2 – *The categories of the orbits*

The geometry associated to the Hamiltonian (5.1) allows us to get a picture of the dynamics around the collinear point L_1 and to establish the types of orbits that a spacecraft can travel.

We proceed to fix a level energy slightly above the critical value at which we have the appearance of a neck; through this passage there exist *transit* orbits between the two primaries. We will also show the existence of *non-transit* as well as *asymptotic* trajectories. These three categories of orbits are found by carefully inspecting the geometry associated to (5.1). Afterwards, we will use Moser's version of Lyapunov's theorem to establish that the flow in a specific region is homeomorphic to the flow obtained in the same region by using the linearized equations of motion ([4]).

Following [4], we consider a region $\mathcal{R}$ setting $H_{linear} = h$ and $|p_1 - q_1| \leq c$ for some constants $h, c > 0$. Within the plane $(p_1, q_1) \in \mathbb{R}^2$, the region $\mathcal{R}$ is bounded by the two lines $p_1 - q_1 = \pm c$. On the other hand, setting $p_2^2 + q_2^2 = 0$ and $p_3^2 + q_3^2 = 0$, the region $\mathcal{R}$ is crossed by the two branches of the hyperbola $p_1 q_1 = h/\lambda$ (see Figure 3). Another hyperbola is given by the expression $p_1 q_1 = d$ with $d < 0$ constant; the two branches are shown in the second and fourth quadrant of Figure 3.

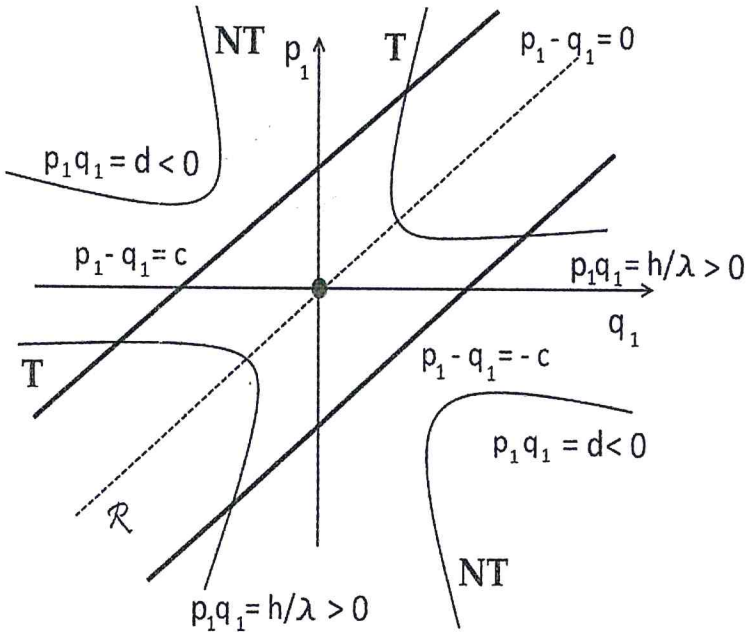

Fig. 3. – The geometry associated to the linearized Hamiltonian (5.1). The saddle point is located at the origin; the region $\mathcal{R}$ is bounded by the thick lines $p_1 - q_1 = -c$ and $p_1 - q_1 = c$. Transit orbits are labeled by T, while non-transit orbits are denoted as NT.

Within the plane (p_1, q_1) shown in Figure 3 with the saddle point located at the origin, we distinguish between three categories of orbits:

(*i*) *asymptotic* orbits, forming the stable and unstable manifolds defined, respectively, by the equations

$$\frac{\omega_2}{2}(p_2^2 + q_2^2) + \frac{\omega_3}{2}(p_3^2 + q_3^2) = h\ , \qquad q_1 = 0$$

and

$$\frac{\omega_2}{2}(p_2^2 + q_2^2) + \frac{\omega_3}{2}(p_3^2 + q_3^2) = h\ , \qquad p_1 = 0\ ;$$

(*ii*) *transit* orbits: determined by the hyperbolic segments $p_1 q_1 = h/\lambda$, where h/λ is a positive quantity and bounded by the lines $p_1 - q_1 = \pm c$;

(*iii*) *non-transit* orbits: determined by the hyperbolic segments $p_1 q_1 = d$, where d is a negative constant.

We refer to Figure 3 for a schematic illustration of these orbits. Such classification suggests to use the transit orbits around the collinear point L_1 to move from one primary to the other. A mission design based upon this strategy will be the content of Section 6.

5.3 – *The center manifold reduction*

When considering the nonlinear flow, the Hamiltonian is composed by the linear part (5.1) to which we add the nonlinear terms, say:

$$(5.2)\quad H_{nonlinear}(p,q) = \lambda p_1 q_1 + \frac{\omega_2}{2}(p_2^2 + q_2^2) + \frac{\omega_3}{2}(p_3^2 + q_3^2) + \sum_{n\geq 3} H_n(p,q),$$

where we assume that the H_n's denote homogeneous polynomials of degree n. A seminal ingredient is now provided by Moser's version of Lyapunov's theorem ([19]), according to which the results found in the context of the linearized system are valid also for the full nonlinear equations. This result allows us to transpose the definition of asymptotic, transit and non-transit orbits also to the nonlinear case.

In order to study the dynamics in the proximity of the collinear point, it is convenient to get rid of the instability associated to the hyperbolic direction, through the so-called *center manifold reduction.* This procedure consists in the implementation of a suitable transformation of coordinates (typically obtained through a Lie series transformation). This normal form aims at removing the hyperbolic direction (see, e.g., [15]) and it allows us to analyze the stable components in the neighborhood of the collinear point.

More precisely, within the linear approximation the center manifold is computed just by setting the hyperbolic coordinates to zero: $p_1 = q_1 = 0$. If we impose that $\dot{p}_1(0) = \dot{q}_1(0) = 0$, whenever $p_1(0) = q_1(0) = 0$, we get that $q_1(t) = p_1(t) = 0$ for any time, due to the fact that the Hamiltonian function is autonomous. Let us now consider the nonlinear problem with Hamiltonian $H = H_{nonlinear}$. Assume that each function

H_n in (5.2) is expanded as a sum of monomials of the form $\chi_{kj} p^k q^j$ for some coefficients χ_{kj}. From Hamilton's equations associated to H in (5.2), namely

$$\dot{q}_i = \frac{\partial H}{\partial p_i}\,, \qquad \dot{p}_i = -\frac{\partial H}{\partial q_i}\,,$$

we need to require that all monomials of the type $\chi_{kj} p^k q^j$ with $k_1 \neq j_1$ are such that $\chi_{kj} = 0$, where we used the convention that $k = (k_1, k_2, k_3)$ and $j = (j_1, j_2, j_3)$.

Let us denote by (p_x, p_y, p_z, x, y, z) the coordinates after the normal form reduction. We denote by $\tilde{H}(p_x, p_y, p_z, x, y, z)$ the transformed Hamiltonian after the center manifold reduction up to the order $N \in Z_+, N \geq 3$, which can be written as follows:

$$\begin{aligned}\tilde{H}(p_x, p_y, p_z, x, y, z) = {} & \lambda p_x x + \frac{\omega_1}{2}(p_y^2 + y^2) + \frac{\omega_2}{2}(p_z^2 + z^2) \\ & + \tilde{H}_3(p_x x, p_y, p_z, y, z) + \tilde{H}_4(p_x x, p_y, p_z, y, z) \\ & + \ldots + \tilde{H}_N(p_x x, p_y, p_z, y, z) + R_{N+1}(p_x, p_y, p_z, x, y, z),\end{aligned}$$

where $\tilde{H}_n$, $n = 3, \ldots, N$, denotes a homogeneous polynomial of degree n, depending on the product of p_x and x, while the function R_{N+1} denotes the remainder of order $N + 1$.

5.4 – *Halo and Lissajous orbits*

After performing the center manifold reduction, we investigate the dynamics which pertains to the center × center part. Due to Lyapunov's center theorem (see, e.g., [13]), the oscillations which occur in the plane of motion give birth to the so-called *planar Lyapunov* trajectories, while the oscillations in the orthogonal direction generate the *spatial Lyapunov* orbits. On each fixed energy level, we also find the *Lissajous* orbits, carrying out an irrational flow (or possibly foliated by periodic orbits) and connecting the Lyapunov families.

Let us now look at the behavior of the system as the energy varies. Assume to start with low values of the energy and let it gradually increase the energy level. Then, the stability character of the orbits varies and bifurcations occur at specific energy levels. At the bifurcation point, new families of periodic orbits are generated. Precisely, the family bifurcating from the planar Lyapunov orbit (namely the outermost orbit in the Poincaré section of Figure 4, left panel) is the so-called *halo* family ([8], see also [9]), which is characterized by the fact that the frequency of the planar Lyapunov trajectory equals the frequency of its vertical perturbation (see Figure 4, right panel). Other bifurcations can be found at higher energy levels (see, e.g., [12], [1]). The energy transition value at the bifurcation can be evaluated on the basis of the graphical results provided by the Poincaré surfaces of section, as provided in Figure 4. An analytical method to estimate the energy level at which the bifurcation occurs has been devised in [3] (see also [1]) by computing a proper resonant normal form. It is remarkable to notice that the analytical results show a very good agreement with the numerical expectation provided by the Poincaré surfaces of section.

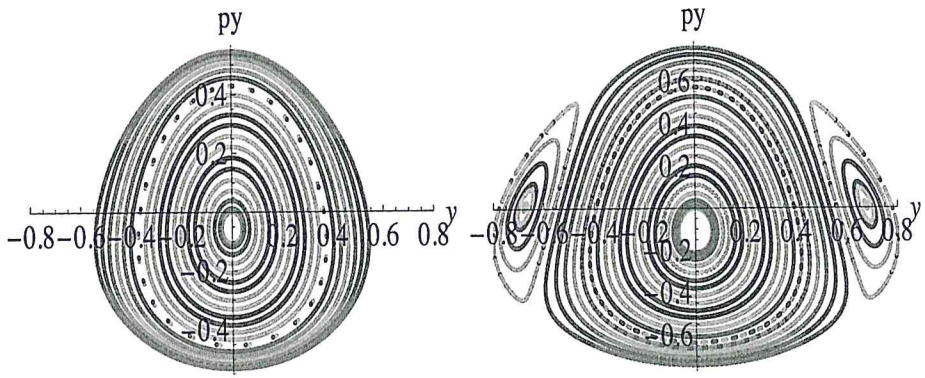

Fig. 4. – Poincaré sections of the center manifold corresponding to L_1 on the plane (y, p_y); the mass-ratio of the primaries is fixed to $1.36 \cdot 10^{-10}$ (this value is of the order of magnitude of an asteroid–Sun mass ratio, compare with [1]). Left panel: $h = 0.3$, the outermost curve corresponds to the planar Lyapunov orbit, while the center of the curves corresponds to the vertical Lyapunov orbit. Right panel: $h = 0.6$, a bifurcation of the planar Lyapunov trajectory generates the halo orbits, corresponding to the left and right lobes appearing in the figure.

6. – Low-cost interplanetary missions

The results of the previous sections allow us to plan travels at low-cost within the Solar system. Being ahead of his time, a mission design was already envisaged by Conley ([4]) and it is sketched in Section 6.1. It will not be necessary to wait many years to appreciate the ideas of exploiting chaos and collinear points to realize low-energy space missions, as described in Section 6.2.

6.1 – *A mission design*

In his visionary paper, Conley ([4]) makes a bridge between his beautiful mathematical approach and an astrodynamical application to design a space mission from Earth to Moon with the following requisites:

(*a*) the cost should be as small as possible;
(*b*) have an easy control and guarantee the stability of the trajectory;
(*c*) try to get as much flexibility as possible.

The first requirement is met by the fact that the spacecraft should move on an energy level just above that of the collinear point L_1. This ensures a minimal fuel consumption, although one needs to be careful that the chaotic character might possibly lead from transit to non-transit orbits. On the other hand, one can use the sensitivity to the choice of the initial conditions to ensure the other two requirements.

The mission design will then be the following: from a loop orbit around the Earth, the spacecraft is given an impulse to be transferred on a transit orbit passing through the neck. Once in the proximity of the Moon, another impulse will be necessary to move the spacecraft on a loop orbit about our satellite. Of course, the whole journey might require a time quite long, at least when compared to other space missions which however request a much larger amount of fuel. For this reason Conley concludes that *one cannot predict how knowledge will be applied.* However, it will suffice to wait only a decade to have the first space mission using Conley's seminal ideas.

6.2 – *In the deep sky*

The orbits around the libration points, known with the acronym of LPOs ("Libration Point Orbits"), have several desirable features in Astrodynamics. From the practical point of view, we mention the following advantages of using LPOs (see [10]):

(*i*) the L_2 point in the Earth-Moon system allows us to have a permanent contact between the Earth and the hidden side of the Moon;
(*ii*) the collinear points of the Earth–Sun system can be reached easily and in a quite inexpensive way;
(*iii*) in the Earth–Sun system, the collinear points L_1 and L_2 provide good sites where to place, respectively, solar and astronomical observatories;
(*iv*) the hyperbolic character of the collinear points makes possible to use the stable/unstable manifolds to transfer a spacecraft to/from the libration points;
(*v*) the low-energy missions around LPOs can be used to provide interplanetary transfers in order, for example, to establish a base on the Moon or Mars, as well as to transport raw material from the other celestial bodies.

Nowadays, the technique of using LPOs for space missions is widely implemented. We give below a small sample of the main missions launched during the last decades, using collinear points, halo orbits and Lissajous trajectories.

(1) The first mission using LPOs was ISEE-3 ("International Sun/Earth Explorer 3"); launched by NASA/ESA in 1978 to study the interaction of the solar wind when crossing the magnetic field of the Earth, it was placed on a halo orbit around the point L_1 in the Earth–Sun system.
(2) SOHO, standing for "Solar and Heliospheric Observatory", was launched in 1995; it is still active and provides very useful space weather predictions, thanks to its location on a halo orbit around the collinear point L_1 of the Earth–Sun system.

(3) WMAP, standing for "Wilkinson Microwave Anisotropy Probe", launched in 2001 it had the ambitious project of measuring the Cosmic Microwave Background Radiation, namely the thermal radiation which occurs as a remnant of the Big Bang. Again, orbits around the Earth–Sun L_2 point and Lissajous trajectories have been used to design the mission plan of WMAP (see Figure 5, top panel).

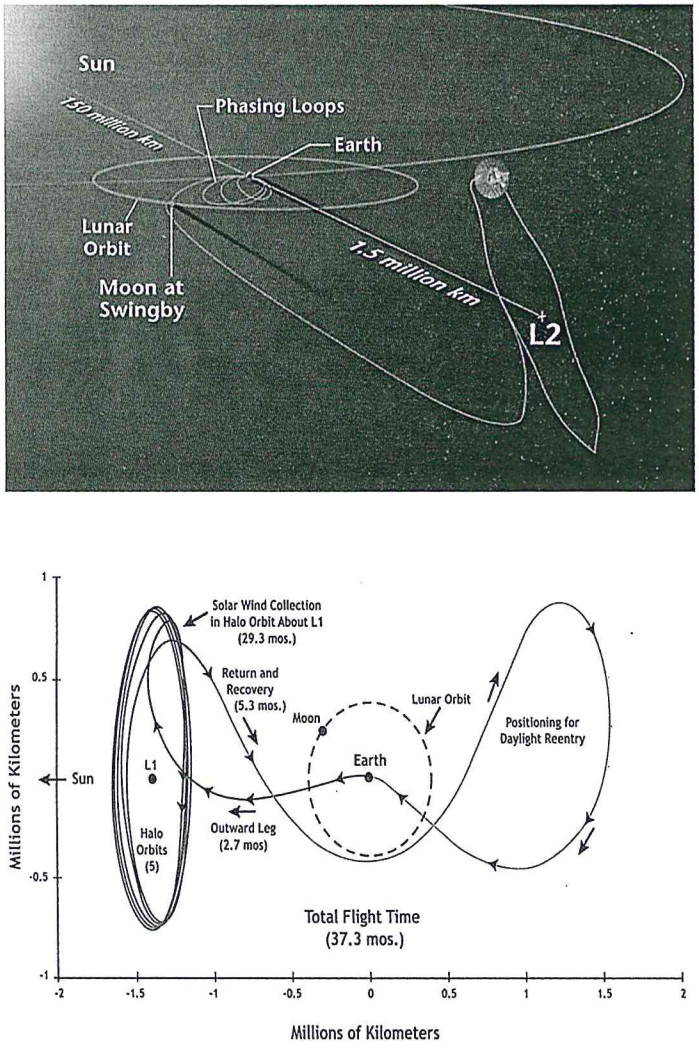

Fig. 5. – The flight plans of WMAP (top panel) and Genesis missions (bottom panel). Credits: NASA/JPL.

(4) GENESIS was launched in 2001 as a sample return mission with the goal of collecting solar wind; after crossing the Earth–Sun point L_1, GENESIS was placed on a Lissajous orbit, before ending on an elliptical orbit about L_1 (see Figure 5, bottom panel). After spending a little more than 2 years collecting solar wind, GENESIS made five halo orbits around L_1, then it started its travel back to the Earth, which included a loop around L_2, just to let it arrive during daytime, thus making easier the recovery of the collected sample.

(5) HERSCHEL-PLANCK: launched in 2009, the Herschel-Planck Space Observatory was placed in orbit around the collinear point L_2 of the Earth–Sun system as a continuation of WMAP with the aim to detect anisotropies of the cosmic microwave background, again bringing us back to the origin of the Universe.

These missions are indeed a tribute to the scientists that worked over the centuries with vivid imagination and deep mathematical insight to pave the space with new dynamical routes.

Acknowledgments. The author deeply thanks Marta Ceccaroni and Giuseppe Pucacco for useful discussions and for critically reading the manuscript.

REFERENCES

[1] S. Bucciarelli, M. Ceccaroni, A. Celletti, G. Pucacco, *Qualitative and analytical results of the bifurcation thresholds to halo orbits*, accepted for publication in Annali di Matematica Pura ed Applicata (2015).

[2] A. Celletti, *Stability and Chaos in Celestial Mechanics*, Springer-Verlag, Berlin; published in association with Praxis Publishing Ltd., Chichester, ISBN: 978-3-540-85145-5 (2010).

[3] A. Celletti, G. Pucacco, D. Stella, *Lissajous and Halo orbits in the restricted three-body problem*, accepted for publication in J. Nonlinear Science (2015).

[4] C.C. Conley, *Low energy transit orbits in the restricted three-body problem*, SIAM J. Appl. Math. **16**, n. 4, 732-746 (1968).